

EIGHTEENTH EUROPEAN ROTORCRAFT FORUM

E - 05

PAPER N° 151

HHC EFFECTS ON HUB AND BLADE LOADS

H.-J. LANGER, R. KUBE
DLR, Germany

September 15-18, 1992

AVIGNON, FRANCE

ASSOCIATION AERONAUTIQUE ET ASTRONAUTIQUE DE FRANCE

HHC EFFECTS ON HUB AND BLADE LOADS

H.-J. Langer and R. Kube

Deutsche Forschungsanstalt für Luft-und Raumfahrt, Institut für Flugmechanik,
Flughafen, D-33 Braunschweig, Germany

1. Abstract

Wind tunnel tests were performed with a 4m diameter hingeless model rotor in order to investigate the influence of different HHC inputs to noise and vibration. The rotor test condition corresponds to a moderate *descent* helicopter flight.

Besides the reduction of both the 4p hub loads (measured by a rotor balance) and the blade vortex interaction (BVI) impulsive noise of the rotor, it was found, that the rotor *trim* condition *changes* under HHC input. This change affects all the six hub components but mainly the rolling and pitching moments.

The magnitude of this 'out of trim' depends on three HHC conditions (frequency input (3,4, or 5p) , magnitude of the control angle, phase of the control angle).

In order to verify this trim effect and to examine loads in the rotating system (e.g. pitch link force, blade bending moments, accelerations, etc.) different sensor signals (strain gauges, accelerometers, piecos) are investigated with and without HHC input. It was found that HHC input can reduce 4p hub loads but increase amplitudes for other harmonics (e.g. 6p hub acceleration). It is also shown that the HHC *input-phase* change the blade tip deflection for nearly *all* harmonics even the 1p. This may influence the directivity of the BVI noise.

The increase or decrease of amplitudes at *some* excitation frequencies depends on the dynamic characteristic of the rotor support. However, the shift of the rotor trim condition and blade tip vibration - which is quite important when feed back control is applied - is a blade or rotor dependent effect caused by blade dynamic and aerodynamic interactions .

2. Notation

s	-	scale factor (2.46)*)
R	-	rotor radius (2m)
σ	-	solidity (0.077)
f_{R0}	-	rotor frequency (17.5Hz)
$-F_z$	-	z-force @ hub or 0p vertical force, in rotor shaft direction ($\approx 3400N$)
c_T	-	$= c_{(-F_z)}$; thrust coefficient (0.0044)

Ma_{Tip}	-	blade tip Mach number (variable, due to const f_{RO})
α_{shaft}	-	rotor shaft tilt (+5.3°)
z_{pp}	-	d^2z/dt^2 ; acceleration in F_z
φ	-	HHC input phase
ψ	-	rotor azimuth phase

*) figures in brackets indicate model data resp. test data

3. Introduction

Higher Harmonic Control (HHC) is a promising tool to decrease vibration and impulsive noise. Reduction of vibration means to decrease $n \cdot p$ hub loads in the fixed axis frame for a n -bladed rotor by means of a suitable control input. Using the classic swashplate control for a four-bladed rotor only three possible higher harmonic controls can be applied. Basis for all is a harmonic excitation of the swashplate four times per rotor revolution using three actuators. A phase lag of $\pm 120^\circ$ among the actuators produce a 3p blade pitch signal, resp. a 5p signal. A 0° phase lag results in a 4p blade pitch. Mixed modes can be applied, too. The control actuators operate all the time with a constant frequency of 4p.

For each HHC input the phase shift between the actuators has to be constant. Not constant is the HHC input phase with respect to the azimuth position of the blades. Shifting this phase can reduce or amplify vibration and/or noise.

Many tests are performed to find out at which HHC phase best results can be achieved for vibration and noise reduction.

All the test data presented here are gathered with a scaled down model rotor of the Bo105 main rotor mounted on the DLR rotor test support.

4. Test Set Up

4.1 Wind Tunnel Tests

Wind tunnel tests were performed with a 4m diameter hingeless rotor in order to investigate the influence of different HHC control inputs to noise *and* vibration [1],[2]. The tests were accomplished in the anechoic test chamber of the DNW using the 8m by 6m open jet .

The rotor revolution was set to 1050 rpm (i.e. 17.5Hz). Test condition for all HHC inputs had been: $v=33\text{m/s}$, $\alpha_{shaft}=+5.3^\circ$ (tilted backward), and $c_T=0.0044$. This condition corresponds to a moderate *descent* Bo105 flight. However, model rotor trim condition was different with respect to the full scale rotor: The model rotor was trimmed to zero hub moments (pitching and rolling) which does not mean that the 1p flapping moment vanishes [3],[4]. Therefore a small tip path plane tilt was present with respect to the rotor shaft. (This is important to know when hub and blade loads have to be interpreted).

4.2 Sensor System

Three main components for data measuring were used for the HHC tests:

1. sensors in the rotating system
2. sensors in the rotor support system
3. microphones and flow related sensors

In addition to some strain gauge sensors in the blade root area (e.g. to measure flapping moment, lagging moment, and torsion moment), three 3-component accelerometers are installed: two in the blade tip (fig.1) and one in the rotor hub, centred around the shaft axis. Blade pitch was measured with high accuracy using a potentiometer strip glued close to the pitch hinge. Pitch link loads were measured using different principles: Two from four are equipped with piezo electric washers, and two with strain gauges.

Measuring in the fixed axis system was mainly performed via a 5-component balance and a torque meter. The balance was calibrated statically with respect to the rotor hub.

As the dynamic characteristic of the rotor was only required with respect to relative values, dynamic calibration of the balance was not performed. Regardless of atmospheric condition all tests were done with 1050rpm.

A z-accelerometer mounted on the rotor hub was used to cross-check the vibration results of the rotor balance with respect to phase and amplification. It was found that the differences between both can be neglected.

In order to generalize vibration effects not caused by the rotor blades, a so called 'inertia compensation' was required: The rotor without blades was tuned to 1050rpm and HHC was applied using sequential control inputs for 3p,4p, and 5p and with 0.4° and 0.8° blade pitch. The phase was scanned with a stepsize of $\Delta\phi=30^\circ$.

Results show, that the relation is *linear* between the HHC input amplitude and the 4p output for accelerations, forces and moments. More details can be found in chapter 5 (results).

4.3 Control and Data Management

HHC was performed for both: open loop tests and closed loop tests. As different sensor signals were used for vibration (7 sensors) and impulsive noise reduction a quite sophisticated hardware architecture was build up for the closed loop tests based on parallel processing. In order to determine the best compromise between noise and vibration reduction a transputer based hardware was necessary to handle the high sampling rate required for the noise signals, the CPU time consuming FFT's (for the acoustic signals), harmonic analysis (to determine the 4p vibration), and synthesis. Hard- and software was described in detail in [2].

Open loop HHC inputs consisted on 3p, 4p and 5p inputs for 0.8° , and 1.2° blade pitch angles. The phase input was varied stepwise by $\Delta\phi=5^\circ$.

The HHC inputs are accomplished using three hydraulic actuators controlled by a transputer system. The actuators are mounted on the upper plate of the rotor balance and are used for rotor trim (i.e. 0p and 1p-control), too.

In order to get the proper HHC output signal at the blade root, it was necessary to apply a controller *compensating the different transfer characteristic of the actuators* [5].

As the actuators perform both - the HHC and trim control - a locking device was installed which 'freeze' a control condition if the difference between nominal control input and actual control output exceeds a preset value.

After a HHC control input (phase and amplitude) was applied, the rotor runs in steady state within a quarter of a revolution. The data of approx. 60 sensor signals (without counting microphone signals) are stored in the time domain for about 25 rotor revolutions. All signals are filtered either with 250Hz (for dynamic signals) or 4Hz (for static signals). This allows a useful frequency range up to the 8th order of the rotor harmonic.

5. Results

The main benefit of HHC concerning vibrations is, that the dominant 4p (and often 8p) forces and moments in the nonrotating axis system become smaller in comparison to vibrations without harmonic control. This was shown in a large number of papers. A good compilation was given in [6].

However, HHC does not only alter the 4p and 8p hub loads (or 3p+5p and 7p+9p in the rotating system). HHC may change the whole frequency spectrum concerning amplitude and phase of the rotor and fuselage, even the static hub loads (i.e. trim condition).

Two reasons contribute to that: Location of the blade bending eigenforms and resonance characteristics of the rotor support structure (consisting on an acoustic treatment of the test rig, the rotor balance, a hydraulic drive motor, and the DNW sting).

5.1 Inertia compensation

In order to find out which part of rotor support vibration comes from the rotor blades and which part comes from the control input of the actuators, a so-called inertia compensation test was accomplished.

Operating the rotor without blades yields dynamic values of hub forces and moments which have to be subtracted from results obtained for HHC inputs *with* blades.

Figure 2 shows a plot of the z-force (perpendicular to the axis of no 1p flapping) measured by the rotor balance for different amplitudes of HHC inputs.

As four force transducers in z direction contribute to the z-force at the rotor hub, the same plots were made for a single sensor: a z-accelerometer mounted on the rotor hub. This sensor shows equivalent results.

The HHC input phase was scanned stepwise for one period. (A 3p HHC input complies with a rotor azimuth range of $\psi=120^\circ$).

The reaction is quite different from the control inputs to the z-force. 3p and 5p cause comparable z-reactions, but differs mainly in phase. 4p HHC input yields a nearly constant output for the whole phase range.

The reason for that is a resonance frequency of the rotor support (i.e. balance) in vertical direction at 105Hz i.e. 6p (fig.3). The system is excited for this frequency due to the 3p and 5p control input in the rotating frame and the 4p (70Hz) in the fixed frame.

Figure 3 shows a sweep up to 150Hz in z-direction for the rotor balance. Resonance peaks are present at many frequencies, however, except the 6p, they have no contribution to the vibration level due to HHC. The smaller peaks are caused by coupling effects due to the unsymmetry of the balance and/or test rig.

The relatively strong 6p z-component (fig. 2) excited at 3p and 5p HHC comes from non-linearities (structural damping) of the support system below the actuators. As the actuators move up and down out of phase at 4p, the support system is excited for all $n \cdot p$. For weak damping, resonance amplification becomes apparent when an eigenfrequency of the system coincides with a multiple of the rotor rotation frequency.

In consequence this means, HHC may cause higher vibrations, if a multiple of the rotor rotational frequency coincides with a rotor support frequency e.g. fuselage frequency.

It will be shown under 5.3 how the described effects influence the vibrational loads when blades are attached.

5.2 Static Hub Loads

Besides the inertia effects of HHC to other than 4p or 8p vibrational loads as described in 5.1 and 5.3 another important effect can be shown: HHC inputs tilt the tip path plane (TPP) of the rotor so that the rotor becomes slightly untrimmed. This effect was monitored during HHC open loop tests.

Shifting the phases of the HHC input, change the static loads at the rotor hub. In addition: the higher the HHC input amplitudes the stronger the changes of hub loads.

Figure 4a and 4b show the influence of the HHC input phase to the mean (or static) hub components. Moments and thrust are plotted for two different 3p amplitudes. The curves clearly show that a decreasing input amplitude decrease the effects to the static moments and thrust, too. The mean value of each curve represents the load value without HHC.

The pitching moment M_y is more influenced by HHC input than M_x because the moment response to a flow change is stronger in lateral than in longitudinal direction.

The thrust varies $\pm 3.5\%$ with respect to the thrust of the baseline case (i.e. without HHC). For a 4p HHC input with 1.2° amplitude, the variation is about $\pm 2\%$.

The derivatives are calculated for the measured test condition ($v=33\text{m/s}$, $\alpha_{\text{shaft}}=+5.3^\circ$, and $c_T=0.0044$):

$$\partial F_z / \partial \theta_{0,7} = -830 \text{ [N/deg]}, \quad \partial F_z / \partial \theta_s = -526 \text{ [N/deg]}, \quad \partial F_z / \partial \theta_c = -36 \text{ [N/deg]};$$

$$\partial M_x / \partial \theta_{0,7} = 25 \text{ [Nm/deg]}, \quad \partial M_x / \partial \theta_s = -127 \text{ [Nm/deg]}, \quad \partial M_x / \partial \theta_c = -226 \text{ [Nm/deg]};$$

$$\partial M_y / \partial \theta_{0,7} = 85 \text{ [Nm/deg]}, \quad \partial M_y / \partial \theta_s = 256 \text{ [Nm/deg]}, \quad \partial M_y / \partial \theta_c = -61 \text{ [Nm/deg]}.$$

Applying these values to the hub loads gives an impression of the possible trim angle change due to HHC.

Variation of F_x (long. force) is smaller than for F_y (lat. force) due to the same reason than for the hub moments (fig. 4c,d). The curve for the 4p and 5p HHC input shows not a clean sinusoidal form which may come from non-linearity effects caused by different sources (e.g. actuator synchronization, control system stiffness etc.).

The following table lists the HHC input phase for minimum vibration and minimum BVI noise (mid-frequency level):

p	Ampl.	min. vibr. @	min. BVI @
3	0.8°	180°	72°
3	1.2°	210°	89°
4	0.8°	156°	147°
4	1.2°	270°	164°
5	0.8°	270°	240°
5	1.2°	318°	225°

Applying this table to the diagrams gives an impression how strong the "untrim" effect can be under HHC.

Figure 5 shows the torque and power change due to a 3p HHC input with 1.2° amplitude. The maximum shift is about 10% with respect to the value without HHC. This change is partly caused by the increase of the blade's drag (increasing the power by ≈5%) and - as in the previous figures - caused by the change of the HHC input *phase*. For 4p and 5p the effect is smaller and for a lower HHC amplitude the power loss is smaller, too.

Due to the location of the 1st blade torsion resonance frequency at about 3.6p, amplification occurs between HHC input and blade response. Figure 6 shows the amplification for 3p, 4p, and 5p of two sensor signals: the blade torsion moment and an accelerometer, mounted at the trailing edge of the blade tip. Despite of the amplification, the 0p hub loads are not influenced for the 4p or 5p HHC input. Therefore the stronger change of the hub loads due to 3p HHC input is assumed to come more from blade bending in flap direction than by changes of the local blade's angle of attack due to blade twist.

The effect of "untrim" due to HHC input was verified by calculations, applying two different wake models: the Mangler method, based on the blade's assumed elliptical pressure distribution and derived from the potential theory, and the Beddoes model standing for a prescribed wake model [7],[8].

Figure 7 shows results from calculations and from measurements. Mangler's method underestimates the change of static thrust due to the HHC 3p input phase. This may come from the relatively simple aerodynamic model applied for the Mangler code.

Beddoes's model overestimates the HHC influence. The possible reason can be the stepsize of azimuth increments used for the calculation ($\Delta\psi=15^\circ$) and/or the applied radius of the vortex core ($r/R=0.003$).

Both calculation methods use equal numbers of eigenforms: three in flap, two in lag, and one in torsion. It was found that the number of eigenforms used has an influence on the trim results, too.

A detailed investigation would be necessary to find out how the different code parameters influence rotor trim caused by HHC.

The rotor 'untrim' caused by HHC is a general rotor phenomena, however, the intensity seems to depend on the dynamic characteristic of the rotor blades i.e. mode shapes.

5.3 Dynamic Hub and Blade Loads

Regarding vibrations, HHC mainly impacts the 4p and 8p dynamic rotor loads in the fixed axis frame. This is true for systems which are resonance free for n-multiples of the rotor frequency. With respect to the performed tests with the DLR test rig this was not the case.

As shown in figure 3, the resonance characteristic of the rotor balance has a peak at 6p. As the main direction of the 6p vibration is in z-direction, the F_z and the z-acceleration reflects the typical amplification.

Figure 8a shows the frequency spectrum of the z-acceleration for the multiples of the rotor frequency up to the 8th order. The sensor was mounted on the rotor hub. The legend indicates five conditions:

Condition 1 presents the base line case (no HHC) with the typical spectrum of the test rig for n rotor harmonics.

For condition 2, HHC is applied with a 3p-phase and 3p-amplitude (for blade pitch) where minimum 4p vibration occurs. Acceleration at 6p is now dominant, even 8p is stronger than without HHC input. This probably comes from the 3p control input in the rotating system, which contributes to the 3p itself and - lessened - the 6p (comparable with a four-bladed rotor producing a 4p and 8p vibration).

Due to the resonance point at 6p the amplification is strong. As for the HHC with blades, the same 3p phase and amplitude are applied without blades. But here the 6p reaction is small (condition 4). Therefore it is assumed that mainly the blades cause the amplification at 6p. However, blade signals (e.g. flap, lag, torsion, pitch link load) for all 8 rotor harmonics do not show a significant change of the amplitudes (except 3p) due to HHC 3p input. But in general exciting forces or moments are higher when blades are attached, so that even a small load change may result in a strong vibration increase at a resonance point.

As shown in section 5.2, HHC input has an effect on the static hub loads. Therefore the spectrum is plotted for a HHC input with minimum 'untrim' effect (condition 4). As expected the bars show an increase in vibration for 4p as well as for 6p.

The same HHC condition but without blades shows a high 6p level (condition 5).

Figure 8b gives a closer look to 6p resonance point of the z-acceleration. Two curves are plotted: one with blades and the other without blades. The 3p HHC input phase has a strong impact on the 6p amplitude and both curves are a very different. Non-linear effects are obvious as there is no constant relation between 3p phase input and output. As damping is very low, a small exciting force yields a heavy reaction. In addition, small dissimilarities among the blades result in different pitch link forces, yielding a 3p and 6p force in the fixed frame.

The 4p and 5p HHC input for minimum 4p vibration have a negligible effect on the 6p, however, the 8p becomes dominant for the 4p HHC input (figure 8c). The reason for that was not identified but may result from the dynamic response of the DNW sting support. Resonance sweeps are performed only up to 80Hz for the DNW sting support.

Besides the amplitude spectrum in the fixed axis system the spectrum in the rotating axis system is of importance, too.

For a 3p amplitude input the spectrum of the blade tip z-acceleration is plotted in figure 9. The sensor is located at the 25% blade chord (see fig. 1). Minimum 4p vibration (in the fixed axis frame) means maximum 3p tip acceleration in the rotating axis frame. Other harmonics are involved showing a significant higher amplitude level mainly in the lower harmonics.

Regarding the first harmonic which is responsible for the rotor trim (i.e. rolling and pitching moment) the bars demonstrate the influence for different 3p phase input. The figure shows that most of the amplitudes are smaller without HHC.

This is also the case for the 4p HHC input which increase - beside the 4p amplitude - the 5th and 8th order amplitude for minimum vibration in the fixed axis frame. However, 5p HHC input do not cause amplification of blade flap harmonics (beside 5p) for minimum 4p vibration.

The conclusion can be drawn that the location of the eigenfrequencies and the mode shapes of the blade - excited by different HHC input frequencies - are the cause for the different amplification of the blade tip deflection.

6. Conclusions

Higher Harmonic control has - besides the benefits of 4p vibration reduction and BVI impulsive noise reduction - some interesting side effects:

=> The 0p hub loads may change depending on the HHC input amplitude and phase. The higher the vibration reduction the higher the change. This 'out of trim' effect is strong for the 3p HHC and less intensive for the 5p HHC. This was validated by calculations, too. However, calculation accuracy is poor with respect to the magnitude, but concerning phase the results show good accuracy. Optimizing the input parameters (azimuth increments, vortex core radius, and number of eigenforms) of the mathematical models (Mangler or Beddoes model) may improve the results.

As the wind tunnel measurements are performed for one fixed c_T and α_{shaft} at a moderate advance ratio of $\mu=0.15$, higher loads and μ 's will result in stronger 'trim' effect due to HHC input. This has to be considered for higher advance ratios and higher load factors.

=> Due to the presence of a resonance point of the rotor balance at 6p, 3p HHC input shows a strong impact on the 6p z-acceleration in the non-rotating frame. Even stronger vibrations occur at the 8th harmonic for a 4p HHC input.

The amplification at the 6th and 8th harmonic seems to be test stand related but is certainly a general problem for all structures when HHC is applied. It is therefore a good recommendation to investigate the dynamic response of a rotor support by means of a ground vibration test.

7. References

1. W.R. Splettstößer et al.: BVI impulsive noise reduction by higher harmonic pitch control: Results of a scaled model rotor experiment in the DNW. 17th ERF, Paper N° 91-61, Berlin, 1991
2. R. Kube et al.: A closed loop controller for BVI impulsive noise reduction by higher harmonic control. AHS, 48th Annual Forum and Technology Display, pp. 819-842, Washington, 1992
3. W. Johnson: Helicopter Theory. Princeton University Press, 1980
4. H.-J. Langer: Interference Effects for a microphone traverse on rotor hub and blade loads. DLR Report IB 111-92/01, 1992
5. G. Lehmann: Untersuchungen zur höherharmonischen Rotorblattsteuerung bei Hubschraubern, DFVLR FB 87-36, 1987
6. P.Friedmann: Rotary-Wing aeroservoelastic problems. Proceedings. International Forum on Aeroelasticity and Structural Dynamics 1991, Aachen
7. T.S.Beddoes: Representaion of airfoil behaviour. Vertica Vol.7 N°2, pp. 183-197, 1983
8. B.v.d.Wall: An analytical model of unsteady profile aerodynamic and its application to a rotor simulation programme. 15th ERF Amsterdam, paper n°12, 1989

8. Figures

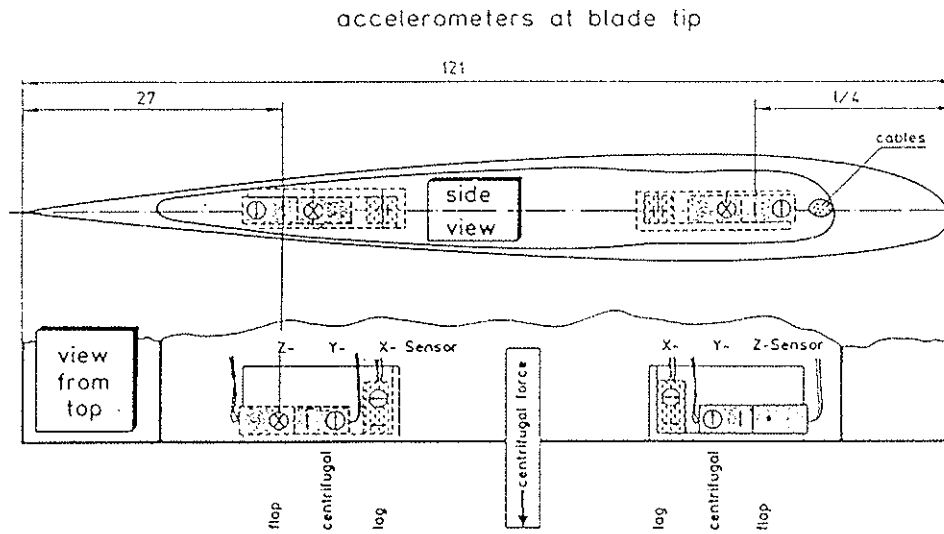


Figure 1: Blade tip instrumentation with accelerometers

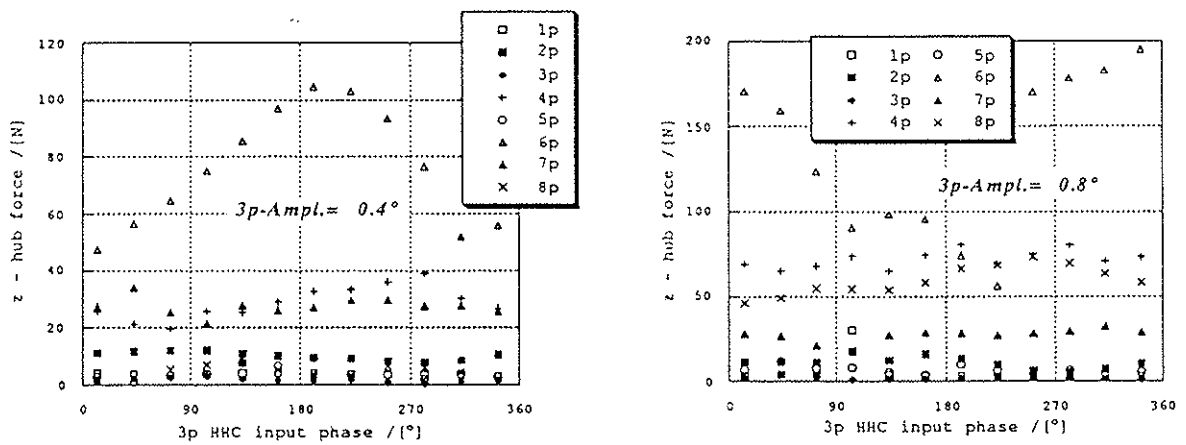


Figure 2a+b: Inertia compensation tests on DNW sting support - hub vertical force

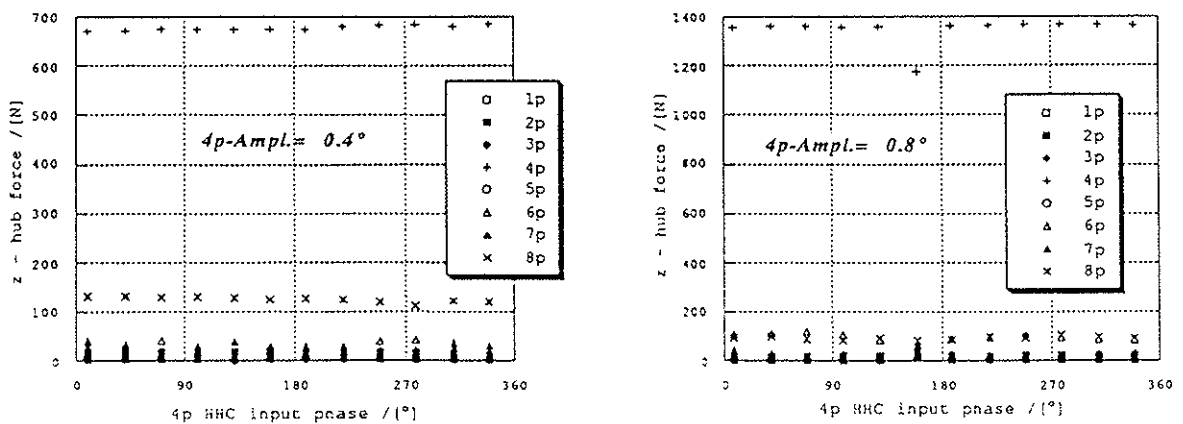


Figure 2c+d: Inertia compensation tests on DNW sting support - hub vertical force

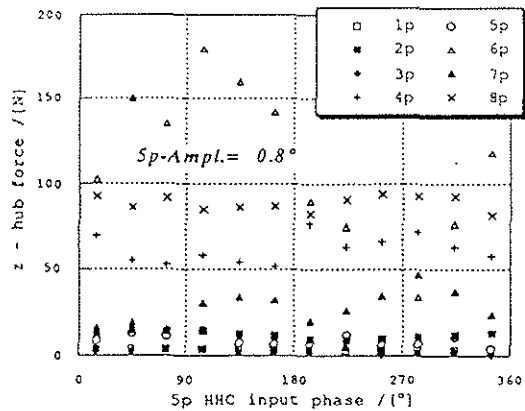
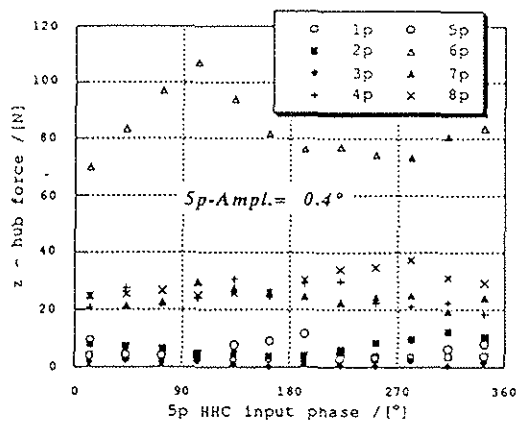


Figure 2e+f: Inertia compensation tests on DNW sting support - hub vertical force

Resonance Characteristic Of The Rotor Balance

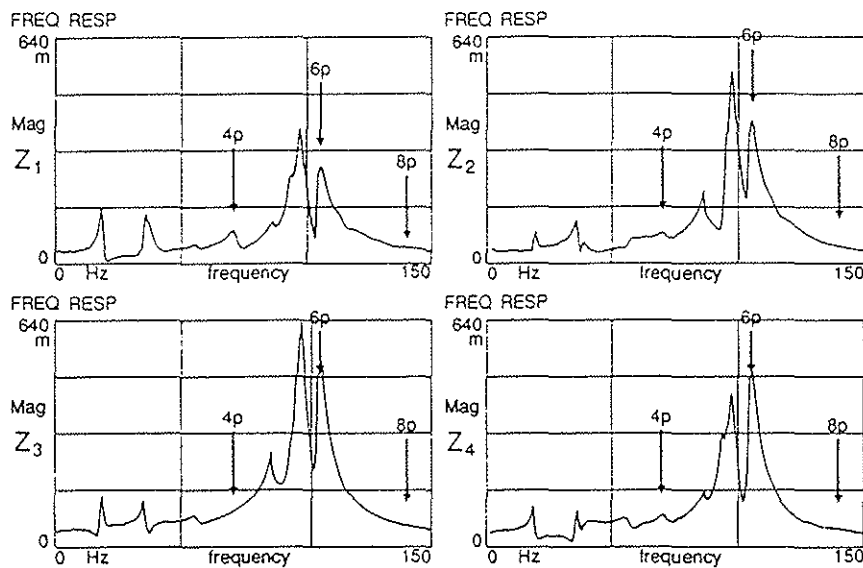


Figure 3: Dynamic Response of four force transducers in z-direction

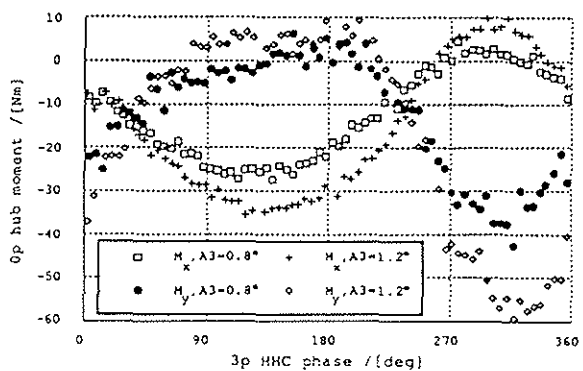


Figure 4a: Hub moments due to 3p HHC input.

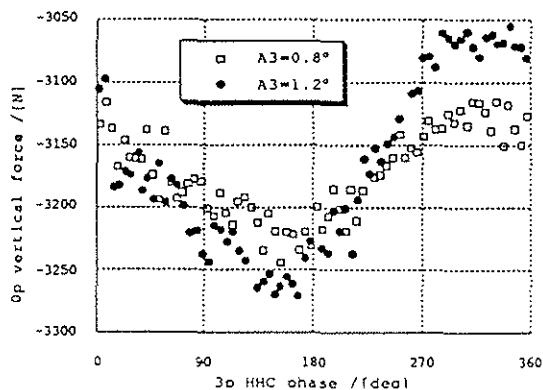


Figure 4b: F_z -shift due to 3p HHC input

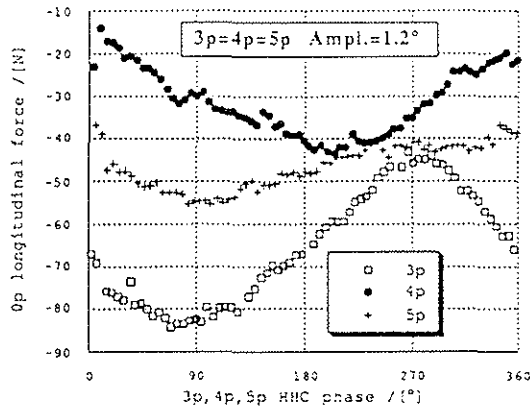


Figure 4c: Effect of HHC frequency on longitudinal force

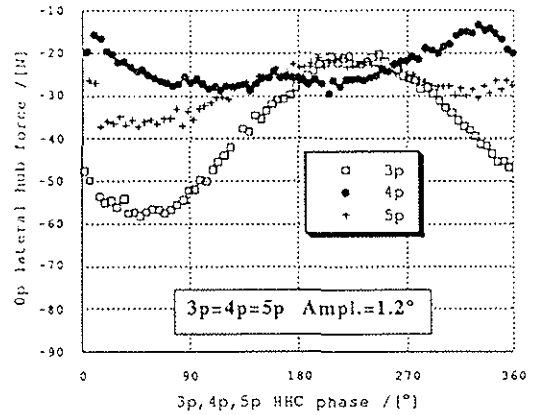


Figure 4d: Effect of HHC frequency on lateral force

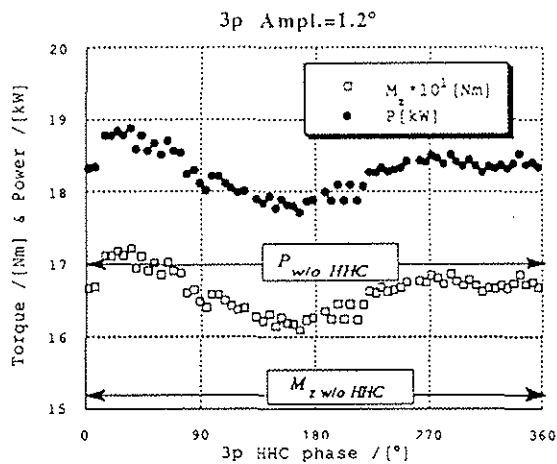


Figure 5 : Influence of a 3p HHC input to 0/rev torque and power

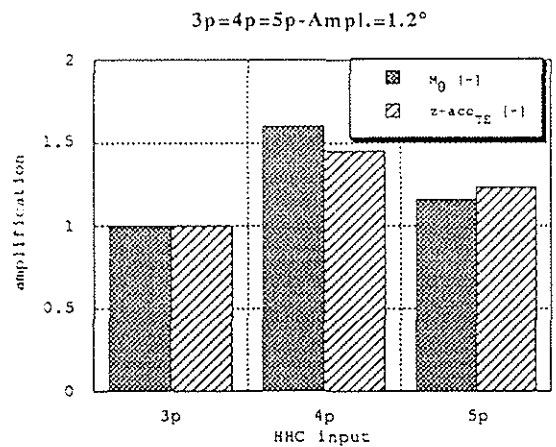


Figure 6: Amplification of blade torsion moment and blade tip acceleration due to 3p,4p, and 5p HHC input at constant amplitude.

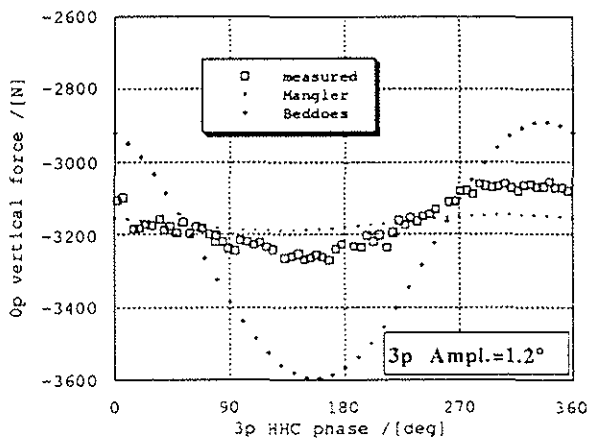


Figure 7: Correlation of measured and calculated trim force

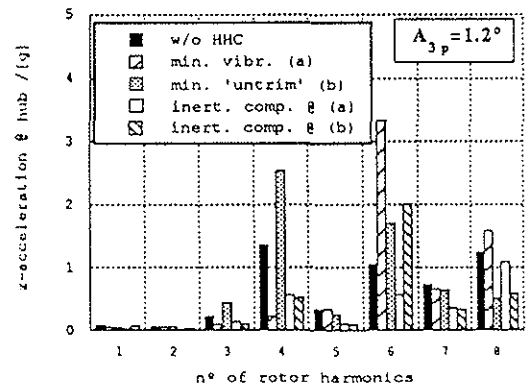


Figure 8a: Frequency spectrum for a 3p HHC input

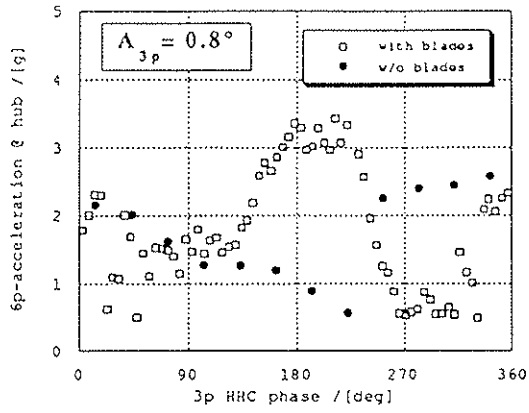


Figure 8b: Blade effect on 6p acceleration

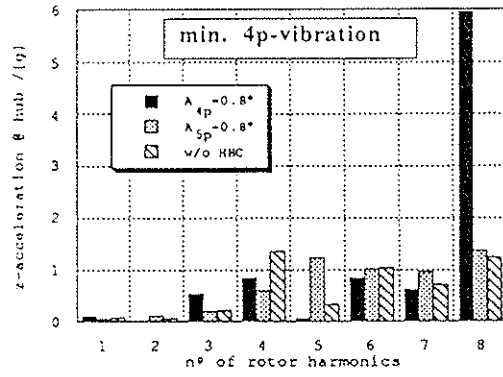


Figure 8c: Frequency spectrum of the hub acceleration to HHC input

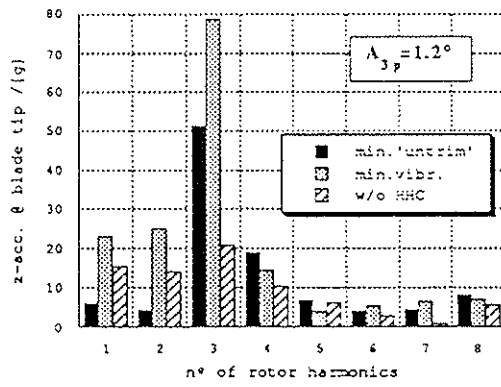


Figure 9: Frequency spectrum for blade tip accelerometer